Development of Super High Resolution Global and Regional Climate Models

Project Representative
Akira Noda Meteorological Research Institute

Authors
Akira Noda *1, Shoji Kusunoki *1 and Masanori Yoshizaki *1
*1 Meteorological Research Institute

Time-slice global warming projections have been performed using a very high horizontal resolution atmospheric general circulation model (AGCM) with a 20-km grid resolution. The dependence of model response on sea surface temperature (SST) prescribed as boundary conditions in the time-slice experiments is investigated. The SST data are obtained from IPCC AR4 global warming simulations with the MRI-CGCM2.3.2 and the MIROC3.2 (hires). The global number of tropical cyclones (TCs) decreases by about 30% in future climate experiments in spite of a large difference in global mean SST increase between the models. However, the change in regional TC frequency is found to be sensitive to local SST changes. In the rainy season, Baiu, over East Asia in summer, precipitation consistently increases over the Yangtze River valley, the East China Sea, and the ocean to the south of the Japan archipelago. It is also found robust that the termination of the Baiu season tends to be delayed until August.

The changes of the Baiu frontal activity due to the global warming are also studied using outputs of a non-hydrostatic regional model with a horizontal grid size of 5 km (5 km-NHM) nested in the 20-km-mesh AGCM. In addition, the model with the horizontal grid size of 1km (1km-NHM) is developed to simulate precipitation qualitatively close to observations, and preliminary results are obtained.

Keywords: global warming projection, high resolution global model, non-hydrostatic cloud resolving model, tropical cyclone, Baiu

1. Subproject 1: Development of a global climate model with a horizontal resolution of 20 km

1.1 Models and experimental design

High horizontal resolution atmospheric general circulation model (AGCM) experiments were realized by adopting so-called the "time-slice" method (Bengtsson et al. 1996; IPCC 2001). This method is defined as the two-tier global warming projection approach using an atmospheric ocean general circulation model (AOGCM) and an AGCM whose horizontal resolution is higher than that of atmospheric part of the AOGCM.

The present time-slice experiments consist of five runs (referred to as AJ, AK, AS, AM and AN) with different sea surface temperature (SST) fields used as the surface boundary condition, i.e., the AJ run with an observed climatological SST (1982-1993, 12-year mean); the AK and AS runs with the observed climatorogical SST plus SST changes from the present (1979-1998, 20 year mean) to the future (2080-2099, 20 year mean) obtained from climate change simulations based on the IPCC SRES A1B emission scenario with coupled atmosphere ocean GCMs, the MRI-CGCM2.3.2 (Yukimoto et al. 2006) and the MIROC (hires), respectively, (see http://www-pcmdi.llnl.gov/ipcc/model_documentation/ipcc_model_documentation.php for detailed information for the models and simulations); the AM and AN runs with simulated SSTs for the present climate and the future climate, respectively, obtained from the MRI-CGCM2.3.2 scenario experiment. The AGCM has been integrated for ten years for the AJ, AK and AS runs, and for twenty years for the AM and AN runs. The experimental designs and names are summarized in Table 1.

1.2 Tropical cyclone

We performed an objective tracking of tropical cyclones (TCs) in the model outputs, basically following the criteria used in previous studies (e.g., Sugi et al. 2002). In addition to our earlier studies, we have investigated sensitivity of the TC climatology to SST conditions in warmer climate simulations.

Table 2 shows the annual-mean number of TCs in the observational data, and in the present-day and future climate simulations for different regions. The global number of TCs in the model decreases by about 30% in the future climate experiments (AK and AS). The result from the AK run has

Table 1 Experimental design

Experiment	Target Period	Sea Surface Temperature (SST)	Year-to-year Variability of SST	Integration Period
AJ	Present	Observed climatology	No	10 years
AK	Future	Observed climatology + ΔSST (MRI-CGCM2.3.2)	No	10 years
AS	Future	Observed climatology + ΔSST (MIROC (hires))	No	10 years
AM	Present	20th Century run by MRI-CGCM2.3.2 from 1979 to 1998	Yes	20 years
AN	Future	IPCC A1B run by MRI-CGCM2.3.2 from 2080 to 2099	Yes	20 years

Observed climatology of SST: 12-year average from 1982 to 1993 by Reynolds and smith (1994)
ΔSST (Model): Change of SST projected with IPCC A1B scenario run (2080-2099) minus 20th-Centurey run (1979-1998)
IPCC: Intergovernmental Panel on Climate Change
MRI-CGCM2.3.2: AOGCM developed by the Meteorological Research Institute
MIROC (hires): AOGCM developed cooperatively by the University of Tokyo, National Institute for Environmental Studies and Frontier Research Center for Global Change

Table 2 Annual-mean number of TC formation in the globe, the Northern and Southern Hemispheres, and six ocean basins. The two-sided Student's t-test was applied to the differences between the values from the present-day simulation and those from the future simulations.

	Latitude	Longitude	Observation 1979-1998 20 years	Model (AJ) Present 10 years	Model (AK) MRI ΔSST 10 years	Model (AS) MIROC ΔSST 10 years
Global	45S-45N	ALL	83.7	78.3	54.8 **	57.1 **
Northern Hemisphere	0 -45N	ALL	58.0	42.9	30.8 **	36.6 *
Southern Hemisphere	0 -45S	ALL	25.7	35.4	24.0 **	20.5 **
North Indian	0 -45N	30E-100E	4.6	4.4	2.1 **	5.8
Western North Pacific	0 -45N	100E-180	26.7	12.4	7.7 **	15.9 #
Eastern North Pacific	0 -45N	180 -90W	18.1	20.5	13.5 *	10.3 **
North Atlantic	0 -45N	90W-0	8.6	5.6	7.5 #	4.6
South Indian	0 -45S	20E-135E	15.4	25.8	18.6 **	19.6 **
South Pacific	0 -45S	135E-90W	10.4	9.4	5.4 **	0.9 **

** Statistically significant decrease at 99 % confidence level.
* Statistically significant decrease at 95 % confidence level.
# Statistically significant increase at 95 % confidence level.

reported in detail by Oouchi et al. (2006). In the western North Pacific Ocean, the regional number of TCs decreases in one of the future experiments (AK), whereas it increases in the other future experiment (AS). In the North Atlantic Ocean, a statistically significant increase is simulated in the AK experiment, but no significant changes in the AS experiment. These results indicate that regional TC frequency is sensitive to local SST conditions.

We have examined TC intensities in terms of maximum surface wind speed. Figure 1 indicates that frequency of intense TCs (e.g., wind speed > 45 m/s) increases globally in both of the future experiments. The global-mean warming of SST was 1.6 K and 3.2 K for the AK and AS experiments, respectively. The intensification of simulated TCs is significantly larger in the AS experiment than in the AK experiment. This reflects the difference in the magnitude of global warming. These new results support our previous study (Oouchi et al. 2006), suggesting a possibility of higher risks of more devastating TCs in a future warmer climate.

1.3 Baiu

Figure 2 shows the geographical distribution of climatological precipitation for July. In the AJ run (b), the model well simulates the observed present climatology (a), although the model tends to overestimate the rainfall amount. In the AM run (c), the model underestimates the observed rainfall amount (a). This is partly due to the discrepancy between simulated SST by the MRI-CGCM2.3.2 and the observed SST. In spite of the large SST differences between AS and AJ, AS and AM, precipitation consistently increases over the Yangtze River valley, the Ease China Sea, and the ocean to the south of the Japan archipelago (d-f). In contrast, the change of precipitation over Korea, the Japan Sea, and Northern Japan scatters among the experiments.

Figure 3 shows the seasonal march of precipitation over the Japan region. In the AJ run (b), the model well simulates the observed northward migration of the Baiu rain band. In the AM run (c), the model also simulates the observed northward migration of the Baiu rain band, although the model

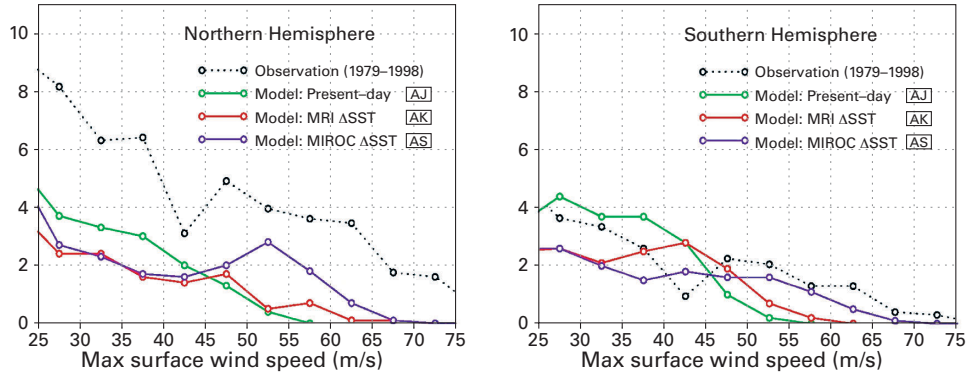

Fig. 1 Frequency distribution of TCs in the Northern and Southern Hemispheres shown as a function of maximum wind speed. The abscissa denotes the peak intensity (maximum surface wind speed), attained in the lifetime of each TC, and the ordinate denotes the annual-mean number of TCs.

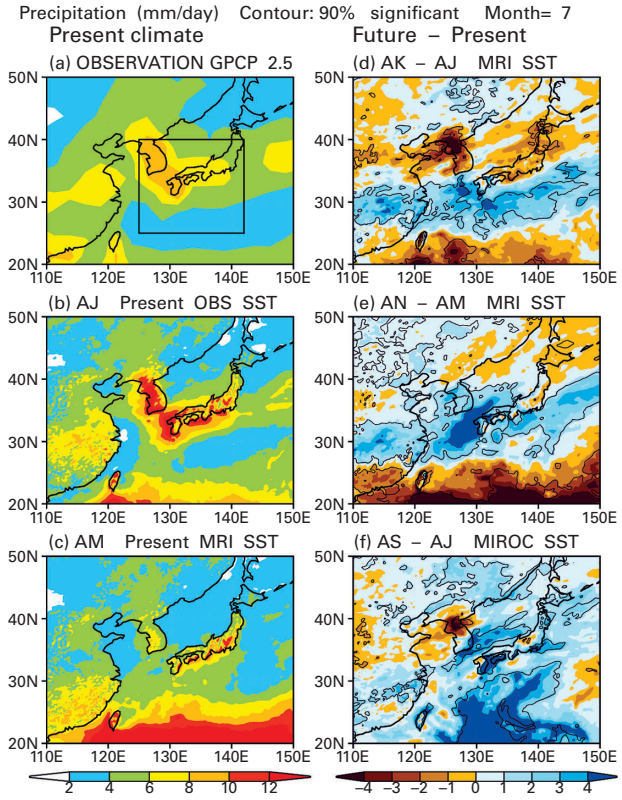

Fig. 2 Climatology of precipitation for July (mm/day). (a) Observed precipitation by Global Precipitation Climatology Project (GPCP, Adler et al. 2003) averaged for 20 years from 1979 to 1998. Horizontal resolution is 2.5 degree. The black box shows the target region for Fig. 3. (b) Model's present climate simulation (AJ). (c) Model's present climate simulation (AM). (d) Change as future minus present climate simulation (AK-AJ). Contours show a 90% significance. (e) AN-AM. (f) AS-AJ.

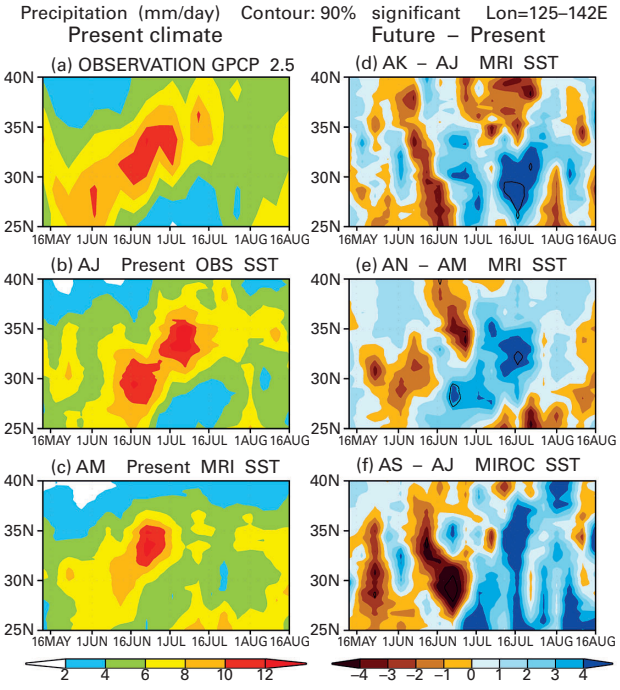

Fig. 3 Time evolution of pentad mean precipitation (mm/day) averaged for 125-142E. From pentad 27(11-15 May) to pentad 46 (14-18 Aug.). The target region is shown by the black box in Fig. 2a. (a) Observation by GPCP data as in Fig. 2a. (b) Model's present climate simulation (AJ). (c) Model's present climate simulation (AM). (d) Change as future minus present climate simulation (AK-AJ). Contours show a 90% significance. (e) AN-AM. (f) AS-AJ.

underestimates the observed rainfall amount (a). Future changes (d-f) consistently show that precipitation increases from the end of July to the beginning of August around the latitudes 30-35N. This indicates that the termination of the Baiu season tends to be delayed until August.

2. Subproject 2: Development of non hydrostatic models (NHMs) with horizontal resolutions of several km

2.1 Extreme precipitation events in the global warming climate (5 km-NHM)

It is interesting how extreme precipitation events that occur only once per several years or more change in the global warming climate. First, we investigate how well the extreme precipitation events are reproduced by the 5 km-NHM.

The upper panel in Fig. 4 indicates occurrence distributions of 12-hourly extreme precipitation events over land in the western Japan. These curves are similar to the Gumbel distribution, which is known as a function describing extreme events in the statistical science. Similar forms are obtained for both 20 km-GCM and 5 km-NHM, but the peak values are different. It is also found that increase rates of peak values are similar between the two models (lower panel in Fig. 4).

Figure 5 shows the changes of return values of extreme precipitation in the global warming climate, simulated by the 5 km-NHM. Here, the return value of extreme precipitation is defined as the rainfall intensity that occurs once every N year, assuming that the occurrence frequency is represented by a Gumbel distribution. In the global warming climate, the extreme precipitation events increase by about 1.15.

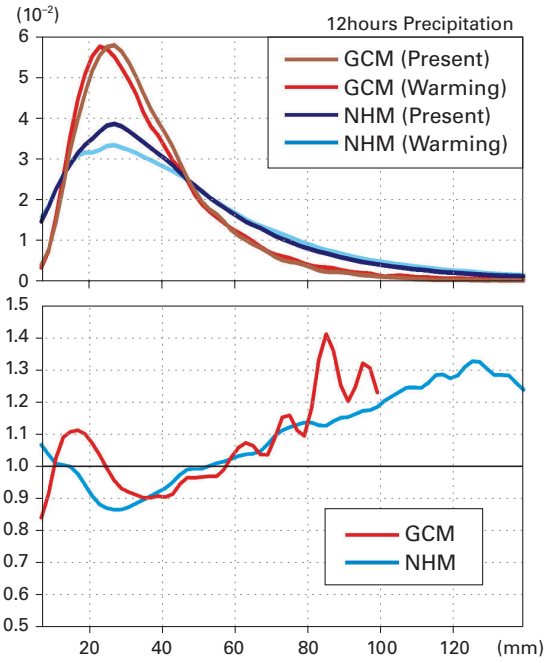

Fig. 4 (Upper figure) occurrence distributions of 12-hourly extreme precipitation events over the land of the western Japan. GCM and NHM mean results of 20km-GCM and 5km-NHM, respectively. (Lower figure) increase rates of peak values of the global warming climate to the present one.

2.2 Development of the 1km-NHM

When compared with observations, the 5 km-NHM underestimated the monthly-mean precipitation in the present climate by about 30 percent. This discrepancy may come from the fact that the precipitation of weak-to-moderate intensity (several - 20 mm/h) was not well represented in the 5 km-NHM. Moreover, the precipitation of weak-to-moderate intensity is mainly produced by cumulonimbi clouds, which have horizontal scales smaller than 5 km. Thus, a smaller horizontal resolution such as 1km (1 km-NHM) is necessary to improve the precipitation of weak-to-moderate intensity by representing realistic convective activity.

However, the 1 km-NHM needs more computer resources in disk space and CPU time than the 5 km-NHM. Therefore, we limited three July cases in the present and global warming climates where heavy precipitation was found over the Kyushu area in the 5 km-NHM, and adopted smaller areas (1600 km × 1200 km), as seen in Fig. 6, compared with the 5km-NHM case. So the spectral boundary coupling (SBC) method is not applied for the 1km-NHM case.

2.3 Preliminary results from the 1km-NHM simulation

Figure 6 shows horizontal distributions of precipitation and surface pressure in the global warming climate simulated with 5 km-NHM and 1km-NHM. The horizontal patterns of surface pressure for the 1km-NHM are well reproduced compared with those for the parent model (5 km-NHM). The detailed structures of cumulonimbi clouds are also simulated by the 1 km-NHM, and the maximum precipitation is enhanced as expected.

Until now, simulations by the 1km-NHM were made only for one case each for the present and global warming climates. Fig. 7 shows the temporal variations of precipitation

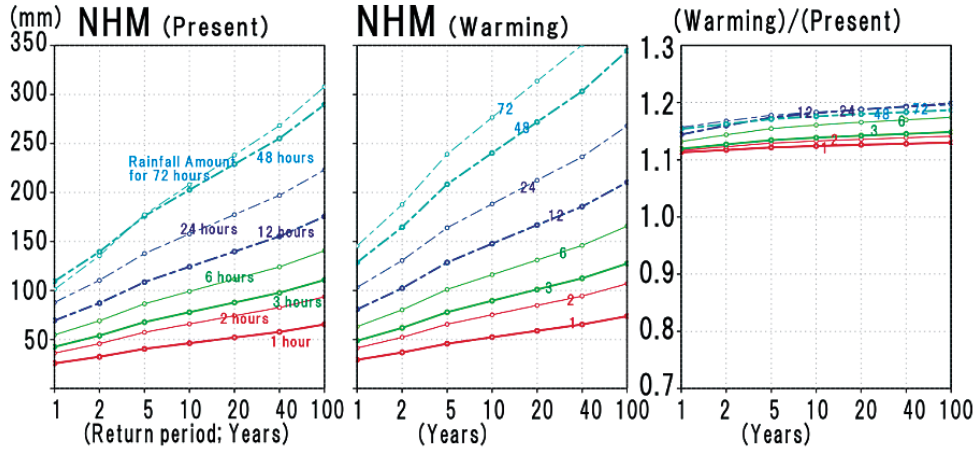

Fig. 5 Return values for1, 2, 3, 6, 12, 24, 48, 72-hourly precipitation as a function of return period over land in the western Japan, simulated by the 5km-NHM. (Left) present climate, (middle) global warming climate, (right) ratios of global warming climate to present one.

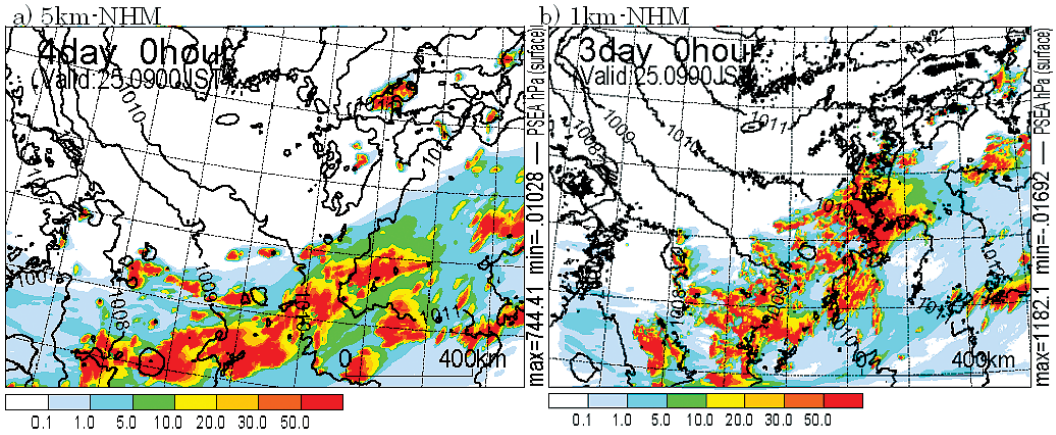

Fig. 6 Horizontal distributions of precipitation (color) and surface pressure (solid lines) in the global warming climate simulated with (a) 5km-NHM and (b) 1km-NHM.

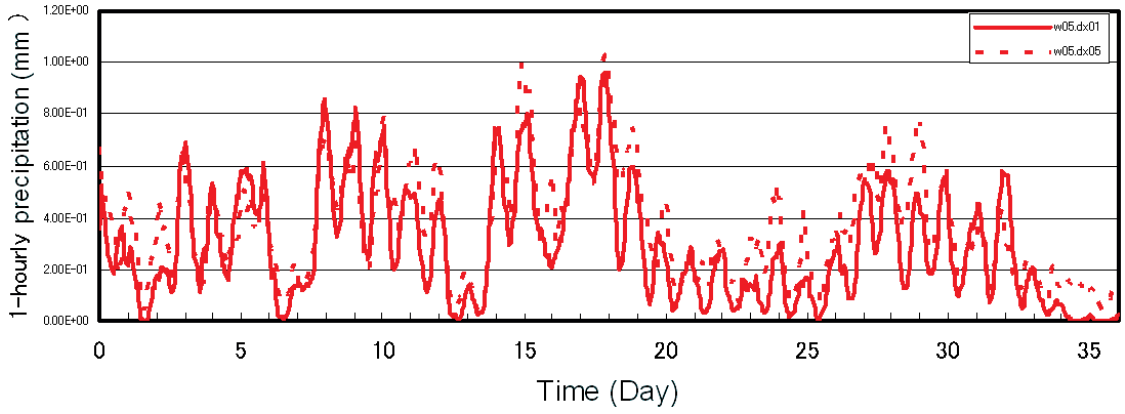

Fig. 7 Temporal variations of 1-hourly precipitation (area average; mm) in the global warming climate. Solid and dashed lines denote 1km-NHM and 5km-NHM, respectively.

in the global warming climate. The peaks of the 1km-NHM correspond well with those of the 5 km-NHM, indicating that the nesting between two models works well. The weak-to-moderate precipitation enhances compared with the intense one for the 1km-NHM, and more realistic reproduction of structure and vertical velocity in the cumulonimbi clouds are also obtained. However, it is found that time-averaged precipitation of the 1km-NHM is a little smaller than that of the 5 km-NHM, contrary to our expectation. At present, these results are preliminary, and we have a plan to calculate more cases in the next fiscal year to investigate the resolution dependency of the NHM.

Bibliographies

Adler, R. F., G. J. Huffman, A. Chang, R. Ferrano, P.-P. Xie, J. Janowiak, B. Rudolf, U. Schneider, S. Curtis, D. Bolvin, A. Gruber, J. Susskind, P. Arkin and E. Nelkin, 2003: The Version–2 Global Precipitation Climatology Project (GPCP) Monthly Precipitation Analysis (1979–Present). J. Hydrometeor., **4**, 1147–1167.

Bengtsson, L., M. Botzet and M. Esch, 1996: Will greenhouse gas-induced warming over the next 50 years lead to higher frequency and greater intensity of hurricanes? Tellus, **48A**, 57–73.

IPCC, 2000: Special Report on Emissions Scenarios. A Special Report of Working Group III of the Intergovernmental Panel on Climate Change. [Nakićenović, N., J. Alcamo, G. Davis, B. de Vries, J. Fenhann, S. Gaffin, K. Gregory, A. Grübler, T. Yong Jung, T. Kram, E. L. La Rovere, L. Michaelis, S. Mori, T. Morita, W. Pepper, H. Pitcher, L. Price, K. Riahi, A. Roehrl, H.-H. Rogner, A. Sankovski, M. Schlesinger, P. Shukla, S. Smith, R. Swart, S. van Rooijen, N. Victor and Z. Dadi (eds.)]. Cambridge University Press, Cambridge, UK.

IPCC, 2001: Climate Change 2001: The Scientific Basis. Contribution of Working Group I to the Third Assessment Report of the Intergovernmental Panel on Climate Change [Houghton, J. T.,Y. Ding, D. J. Griggs, M. Noguer, P. J. van der Linden, X. Dai, K. Maskell and C. A. Johnson (eds.)]. Cambridge University Press, Cambridge, United Kingdom and New York, NY, USA, 881pp.

Mizuta, R., K. Oouchi, H. Yoshimura, A. Noda, K. Katayama, S. Yukimoto, M. Hosaka, S. Kusunoki, H. Kawai and M. Nakagawa, 2006: 20-km-mesh global climate simulations using JMA-GSM model – mean climate states –. J.

Meteor. Soc. Japan, **84**, 165–185.

Oouchi, K., J. Yoshimura, H. Yoshimura, R. Mizuta, S. Kusunoki and A. Noda, 2006: Tropical cyclone climatology in a global-warming climate as simulated in a 20 km-mesh global atmospheric model: Frequency and wind intensity analyses. J. Meteor. Soc. Japan, **84**, 259–276.

Sugi, M., A. Noda and N. Sato, 2002: Influence of the Global Warming on Tropical Cyclone Climatology: An Experiment with the JMA Global Model. J. Meteor. Soc. Japan, **80**, 249–272.

Yoshimura, H. and T. Matsumura, 2005: CAS/JSC WGNE Research Activities in Atmospheric and Ocean Modeling, **35**, 3.27–28.

Yukimoto, S., A. Noda, T. Uchiyama, S. Kusunoki, and A. Kitoh, 2006: Climate changes of the twentieth through twenty-first centuries simulated by the MRI-CGCM2.3. Pap. Meteor. Geophys. **56**, 9–24.

高精度・高分解能気候モデルの開発

プロジェクト責任者
野田　彰　気象研究所
著者
野田　彰*1，楠　昌司*1，吉崎　正憲*1
＊1　気象研究所

20kmメッシュ全球気候モデルを使用し、タイムスライス法による地球温暖化予測実験を行った。

まず気象研究所大気海洋結合モデルMRI-CGCM2.3によりIPCCの排出シナリオA1Bを与え、海面水温(SST)を2100年まで予測した。SSTの年々変動の無い実験としては、現在気候の気候値SST(1982-1998年平均)を20km格子全球モデルに与え、現在気候の10年間の再現実験を行った(AJ実験)。MRI-CGCM2.3予測した将来(2080-2099年平均)のSSTと20世紀再現実験(1979-1998年平均)のSSTの差を、現在気候の気候値SSTに加え、温暖化時のSST(年々変動なし)とした。これを20km格子全球モデルに与え、2090年頃に相当する温暖化時の10年間の予測を行った(AK実験)。同様の将来予測を、温暖化時昇温が大きい他の大気海洋結合モデルMIROCを用いて行った(AS実験)。

SSTの年々変動がある現在気候実験としては、MRI-CGCM2.3による20世紀再現実験のSSTを20km格子全球モデルに1979-1998年の20年間与えた(AM実験)。将来予測は、MRI-CGCM2.3によるA1Bシナリオによる温暖化実験のSSTを20km格子全球モデルに2080-2099年の20年間与えた(AN実験)。

AKとAN実験のSSTの違いは小さいが、AS実験のSSTの全球平均昇温量は、AK, AN実験の約2倍である。20km格子全球モデルによる予測結果が、与えるSSTにどう依存するか調べた。

熱帯低気圧は、AK, AN, ASのいずれの温暖化実験でも全球的な発生数が減少した。一方、北西太平洋・北大西洋など海域別での熱帯低気圧発生数については、実験間に違いが見られ、下部境界条件として与えた温暖化SSTの地域的な分布の違いに依存することが示された。熱帯低気圧を強度別に解析したところ、海上／地上での最大風速が45m/sを超えるような強い熱帯低気圧は、AK, AN, ASのいずれの温暖化実験でも増加していた。この傾向は、全球的な昇温の大きいAS実験の方がより顕著であった。これらの結果は、地球温暖化の進行により、強い熱帯低気圧による自然災害が深刻化する可能性があるというこれまでの研究結果を支持している。

梅雨については、AK, AM, ASのいずれの実験も中国大陸の揚子江付近、東シナ海、日本の南海上で降水量が増加する。一方、朝鮮半島、日本海、北日本では降水量の変化傾向が実験によって異なった。梅雨明けが8月にまで遅れる傾向は、どの実験でも顕著であった。

20kmメッシュ全球気候モデルの結果を側面境界値として与えることにより、水平解像度5kmの非静力学雲解像モデルを用いたタイムスライス法による地球温暖化予測実験を、現在気候、温暖化実験それぞれについて10年間の実験行ってきた。その実験結果を用いて、地球温暖化による梅雨前線活動の変化について調査した。その結果、西日本を中心に梅雨前線の活動が活発となり降水量が増加、特に集中豪雨については九州地方で約7割も増加することがわかった。これらの結果はIPCC第4次報告に貢献するように成果を発表した。また、極端現象の降水頻度について調査したところ、統計的におよそガンベル分布に従うことがわかった。そして、より観測に近い降水量を得るために、水平解像度を1kmとする雲解像モデルを開発した。水平解像度5kmの実験では、現在気候実験の降水量は実際に観測されているものより降水量が少ないバイアスが見られたが、水平解像度1kmの実験では弱い雨の表現が改善され、より現実に近い予備的な結果を得た。今後さらに計算例を増やしてより詳細な解析を行う予定である。

キーワード：地球温暖化予測，高分解能全球大気モデル，雲解像モデル，梅雨，台風